Applied Geochemistry 85 (2017) 201–208

Contents lists available at ScienceDirect

Applied Geochemistry

journal homepage: www.elsevier.com/locate/apgeochem

Radionuclide pollution inside the Fukushima Daiichi exclusion zone, part 1: Depth profiles of radiocesium and strontium-90 in soil

Brett L. Rosenberg [a], Joseph E. Ball [a], Katsumi Shozugawa [b], Gunther Korschinek [c], Mayumi Hori [d], Kenji Nanba [e], Thomas E. Johnson [a], Alexander Brandl [a], Georg Steinhauser [f,*]

[a] Colorado State University, Environmental and Radiological Health Sciences, Fort Collins, CO 80523, United States
[b] Graduate School of Arts and Sciences, The University of Tokyo, Meguro-ku, Tokyo, Japan
[c] Physik Department, Technische Universität München, D-85748 Garching, Germany
[d] Komaba Organization for Educational Excellence (KOMEX), The University of Tokyo, Meguro-ku, Tokyo, Japan
[e] Institute of Environmental Radioactivity, Fukushima University, Fukushima 960-1296, Japan
[f] Leibniz Universität Hannover, Institute of Radioecology and Radiation Protection, D-30419 Hannover, Germany

ARTICLE INFO

Article history:
Received 31 January 2017
Received in revised form
2 June 2017
Accepted 5 June 2017
Available online 8 June 2017

Editorial handling by Prof. M. Kersten.

Keywords:
Fukushima nuclear accident
^{137}Cs
^{90}Sr
^{3}H (tritium)
^{60}Fe
Soil

ABSTRACT

In June 2013 and July 2014, soil samples were collected from unremediated locations within Fukushima prefecture, with special focus on the Fukushima exclusion zone. The soil samples were analyzed for radiocesium by gamma spectroscopy, and then ^{90}Sr by liquid scintillation counting (LSC) after ion specific extraction chromatography. Activity concentrations are compared between sampling years, sampling sites, and soil layers, revealing a general downward trend in activities but also some inconsistencies. Maximum activity concentrations of ^{137}Cs in soil were found in close vicinity of the gate of Fukushima Daichi Nuclear Power Plant and reached up to 10^{6} Bq·kg^{-1} in 2013. Thirteen months later, these maximum levels were lower by a factor of at least 5. Activity ratios of ^{90}Sr/^{137}Cs were usually around $2 \cdot 10^{-4}$, but locally increased to the 10^{-3} range, and in one spot even to the 10^{-1} range. Finally, attempts were made to analyze rare radionuclides in environmental samples from this area, in particular tritium (^{3}H) and ^{60}Fe, however no traces were found in the vegetation and soil samples, respectively.

1. Introduction

On March 11, 2011, a major nuclear accident occurred in Japan after a gigantic tsunami had hit the Fukushima Daiichi nuclear power plant (NPP) and destroyed the emergency cooling facilities of the reactors. Major releases of volatile radionuclides, only exceeded by the Chernobyl nuclear accident in 1986 (Steinhauser et al., 2014), caused significant radionuclide contamination in the vicinity of the Fukushima Daiichi NPP. This fact forced Japanese authorities to permanently evacuate a distinct strip of land northwest of the NPP, which we refer to as the exclusion zone. It has a length of about 40 km and a maximum width of about 10 km (Yoshida and Takahashi, 2012). Radiocesium (^{134}Cs, $T_{1/2} = 2.1$ y and ^{137}Cs, 30.1 y) concentrations and migration in soils in Japan following the nuclear accident have been analyzed extensively (Hashimoto et al., 2013; Kinoshita et al., 2011; Koarashi et al., 2017, 2012a, 2012b; Matsunaga et al., 2013; Nakanishi et al., 2014; Ota et al., 2016; Saito et al., 2015; Yasunari et al., 2011). However, the amount of information available on ^{90}Sr ($T_{1/2} = 28.8$ y) in soils and other environmental media following the nuclear accident at Fukushima Daiichi NPP is not nearly as elaborate (Casacuberta et al., 2013; Fujimoto et al., 2015; Kavasi et al., 2015; Kubota et al., 2015; Povinec et al., 2012; Shozugawa et al., 2016; Steinhauser et al., 2013, 2015; Tanaka et al., 2014; Yamamoto, 2012). Potential reasons for this are the difficulties and amount of (radiochemical) labor associated with separating and quantifying ^{90}Sr as well as the fact that radiostrontium was released in the course of this accident in much smaller amounts (Steinhauser, 2014).

Strontium is an alkaline earth metal with chemical properties related to calcium. The fission product ^{90}Sr is a pure beta-emitting

* Corresponding author.
E-mail address: steinhauser@irs.uni-hannover.de (G. Steinhauser).

http://dx.doi.org/10.1016/j.apgeochem.2017.06.003
0883-2927/

radionuclide. Furthermore, its daughter ^{90}Y is also a beta-emitting radionuclide with a half-life of 64 h. Whereas the maximum energy of the ^{90}Sr beta particle is 0.55 MeV (0.20 MeV average energy), the maximum energy of its daughter is 2.28 MeV (0.93 MeV average energy). Within three weeks, these two radionuclides will reach secular equilibrium, effectively doubling the number of beta emissions. The hazards associated with ^{90}Sr are its tendency to localize to the bone and increase the risk for leukemia or skeletal cancer. For safety, food products following the Fukushima Daiichi NPP accident were routinely screened for gamma-emitting radionuclides (^{131}I, ^{134}Cs, and ^{137}Cs). Strontium-90 was rarely monitored but (initially) assumed to exhibit activity concentrations of not more than 10% of the respective ^{137}Cs activity (Hamada and Ogino, 2012; Merz et al., 2013, 2015).

Strontium has an observed coordination number 8 and can therefore undergo isomorphic substitution with Rb^+, Ba^{2+}, K^+, Ca^{2+}, and Na^+ (Essington, 2005). The affinity of Sr to clays is much less pronounced than the affinity of cesium. The high affinity of Cs^+ is mostly due to the very weak bond between Cs^+ and its coordinating H_2O ligands, resulting in a rather small hydration radius. Strontium, in contrast, has a strongly bound hydration sphere and is hence less prone to interact with clays in presence of smaller ("harder") competing cations. However, Jeong et al. (1996) found that Sr can undergo ion exchange with interlayer K^+, Ca^{2+}, and Mg^{2+} in illite and smectite clays, although its sorption is dependent on pH as it increases with increasing pH. Higher pH levels (in presence of HCO_3^- ions) results in precipitation of $SrCO_3$ (Jeong et al., 1996), however such conditions seem to apply rather rarely in the Japanese environment.

Cesium, as an alkali metal, exclusively occupies oxidation state (+1) (Bostick et al., 2002; Rosso et al., 2001). Its ionic size and radius ratio with oxygen, however, do allow it to undergo isomorphic substitution with Rb^+, Ba^{2+}, and K^+ that are bound in minerals with coordination number 12 (cuboctahedron) geometry (Essington, 2005). By extended X-ray absorption fine structure spectroscopy (EXAFS), the Cs − O bond distances have been measured between 3.2 Å and 4.3 Å. The shorter distance has been associated with outer-sphere complexes, in which the Cs ion is still hydrated. The longer distance has been associated with less mobile inner-sphere complexes with siloxane groups either at frayed edge sites or within the interlayer (Bostick et al., 2002).

The trapping of Cs in interlayer sites by heating or desiccation can result in significant retardation of the leaching of Cs (Essington, 2005; Rosso et al., 2001). Rosso and colleagues discuss how opening the interlayer of muscovite promotes the diffusion of K out of the interlayer space and consequent diffusion of Cs into the interlayer and the dehydration of the Cs ion, collapsing the interlayer. The stronger the negative charge of the interlayer, the more favorable the exchange (Rosso et al., 2001). Coleman and colleagues, however, identify K^+ and NH_4^+ ions as effective Cs^+ ion exchangers for montmorillonite, illite, kaolinite, and vermiculite (Coleman et al., 1963).

Literature teaches us that the sorption and migration behaviors of cesium and strontium are dominated by several equilibria-building factors. In the present study, we attempted to study the natural migration behavior of major radioactive contaminants, $^{134,137}Cs$ and ^{90}Sr, in the Fukushima exclusion zone. In June 2013 and July 2014, soil samples were collected from unremediated locations from Fukushima prefecture, with special focus on the Fukushima exclusion zone. The aim of this study was to analyze radiocesium and ^{90}Sr activity concentrations in soil drill cores (down to 15 cm depth) in June 2013 and 13 months later. The period of 13 months may be too short to draw definitive conclusions for the migration behavior, but it may be a first valuable data set for such studies.

In this pilot study, we also dedicated some efforts to the search for "forgotten" radionuclides, in particular ^{60}Fe and ^{3}H (tritium) (Steinhauser, 2014). Tritium, as one of the most volatile reactor nuclides, is subject for release upon venting of a damaged reactor and fuel meltdown as well as in the release of contaminated waters. Although it has a relatively long half-life (12.32 y), it is characterized by high mobility as a constituent of tritiated water (HTO). Tritium is also responsible for a major nuclear waste problem at the FDNPP site: contaminated cooling water. While foreign materials (cations, anions and even neutral compounds) can be removed from the cooling water by chemical means (Shozugawa et al., 2016), HTO cannot (Normile, 2014). Tritium is produced as a ternary fission product of ^{235}U and ^{239}Pu as well as an activation product in the cooling water, following the nuclear reaction $^{2}H(n,\gamma)^{3}H$. Indeed, two studies on environmental samples taken soon after the accident revealed elevated ^{3}H levels (Kakiuchi et al., 2012; Matsumoto et al., 2013).

A similarly "forgotten" radionuclide is radioiron. Traces of short-lived ^{59}Fe ($T_{1/2} = 44.5$ d) were found in the early aftermath of the accident (Shozugawa et al., 2012). Iron-60 might be formed either at low concentrations by nuclear fission or most likely as activation product on iron or steel components within the neutron flux of a reactor (TU Munich, 1997). Since ^{59}Fe is not produced by nuclear fission, it can only be an activation product on iron or iron containing components within the neutron flux of a reactor. Since it is unclear, which components were released into the environment (causing the detections of ^{59}Fe in 2011), it was warranted to search for long-lived ^{60}Fe ($T_{1/2} = 2.6$ My) in the environment. Iron-60 is likely produced by neutron capture of the relatively short-lived activation product ^{59}Fe. This is a rather unlikely nuclear reaction in areas with low neutron flux (e.g., the pressure vessel), but it becomes more likely with increasing neutron flux densities (e.g., iron deposits on the surface of the fuel rods). A finding of ^{60}Fe would hence be indicative of the release of activated iron from the close vicinity of the fuel rods, in particular the scaling on the fuel rod surface. Presence or absence of this nuclide would hence reveal forensic evidence on the source of the activated iron that was found soon after the FDNPP accident.

2. Materials and methods

2.1. Sampling sites, sample collection and preparation

Two sampling campaigns for soil from inside the Fukushima exclusion zone were conducted in June 2013 and July 2014, respectively. Soil samples were collected at the locations outlined in Table 1. In 2013, one core was taken per site; in 2014 two cores were taken per site (only in location D, a site with very high dose rate levels, three cores were taken). An AMS™ soil core auger was used to collect the top 15 cm of soil in a plastic liner (15 cm length, 5.7 cm diameter) on several locations. The auger is manually driven into the soil and removed with the soil core inside the liner. Then, airtight lids were attached to the openings of the liner tube. This was the methodology of choice for these sampling campaigns because access to the exclusion zone was granted only for limited time and hence required a rapid method of sampling. Driving the soil core auger down to a depth of 15 cm may cause some slight disturbance of the soil layers; however, experiments conducted at Leibniz Universität Hannover showed that these systematic errors by relocation of radionuclides from upper layers to lower layers were <5%. Prior to further processing, the samples were deep-frozen in the lab and sliced into 2.5 cm segments using a saw. The saw blade was thoroughly decontaminated after every cut. It was attempted to repeat sampling 13 months after the first sampling at the exact same locations, however, this was not entirely

Table 1
Fukushima sample descriptions from June 2013 and July 2014. The order represents the locations from north to south.

Site code	Distance to NPP (km)	Site description	GPS coordinates 2013	GPS coordinates 2014
A	32.7	Iitate Village	37.61270 N 140.74905 E	N/A
B	16.2	Odaka Minami Soma	37.56556 N 140.99194 E	37.565961 N 140.992462 E
C	8.5	Chimeiji	37.49556 N 141.00139 E	37.495397 N 141.001808 E
D	1.5	Okuma Town	37.41742 N 141.01012 E	37.417534 N 141.010255 E
E	1	Okuma Town	37.41770 N 141.01510 E	37.417783 N 141.014911 E
F	0	FDNPP Entrance Gate, MP7	37.41736 N 141.02329 E	37.415693 N 141.026747 E
G	4.1	4.1 km from FDNPP	37.38854 N 141.00825 E	37.388553 N 141.008240 E
H	12	Fukushima Daini NPP	37.3147 N 141.01325 E	N/A

possible because the sampling locations at Iitate Village and Fukushima Daini were not accessible in 2014. Also, some sites could not be sampled in 2014 due to the wet terrain. In June 2013, some random vegetation samples (e.g., grass, dandelion) were taken at the sampling sites to search for tritium.

2.2. Geological setting and geochemical implications

The geological setting of the sampling locations is shown in Fig. 1. The figure shows that all samples were taken in locations of marine or non-marine sediments. These sediments are likely dominated by the weathering products of the surrounding Abukuma granite formations. Cationic radionuclides such as Cs^{+} or Sr^{2+} are susceptible to cation exchange processes on various geological materials. These ion exchanging materials primarily include clay minerals (Davey and Scott, 1956) but also silica (Steinhauser and Bichler, 2008). Clay minerals such as Ca-montmorillonite and illite are possible alteration/weathering products of granitic rocks (Dawood and Abd El-Naby, 2001). Especially Cs ions show strong interaction/retention with clay minerals, especially illite or weathered micaceaous minerals (Zaunbrecher et al., 2015). On the one hand, sorption takes place at frayed edge sites of the clay mineral (Kim et al., 2006); on the other hand, illite layers tend to collapse upon uptake of little hydrated cesium into the interlayers and after replacement of hydrated calcium ions (Benedicto et al., 2014).

2.3. Radiocesium analysis

Gamma spectrometry is the method of choice for the analysis of radiocesium in environmental samples. For the cores sampled in 2013, the analysis was conducted with an ORTEC™ 364 cm^3 high-purity germanium (HPGe) detector with a 0.76 mm Be window and 2.32 keV resolution at the 1332 keV ^{60}Co peak (87.4% relative efficiency). For the soil samples taken in 2014, an HPGe detector with 25% relative efficiency and resolution of 1.80 keV at the 1332 keV ^{60}Co peak was used.

Soil core sections were measured in moist state for variable times to ascertain radiocesium content so that a measurement uncertainty due to counting statistics of <10% (in most cases <5%) could be achieved. The samples were placed within a corner of the lead shielding chamber at one-half of the detector height and a distance of 12 cm to the detector. This far-away geometry was chosen to minimize the potential for random coincidence, geometric fluctuations, and high dead time. Spectra were checked for potential peak summation of the 605 and 795 keV peaks of ^{134}Cs, but, thanks to the far-away geometry, none were found. Peaks used for the evaluation were the 662 keV peak of ^{137}Cs and 795 keV of ^{134}Cs. Measurement times and masses are presented in Table S1 (radiocesium) and Table S2 (^{90}Sr), respectively, in the Supporting Information.

For calibration and establishment of an energy-dependent efficiency curve, a multi-radionuclide efficiency calibration standard was created using Eckert & Ziegler™ multi-radionuclide standard (no. 1701–68, reference date December 1, 2013). It was soaked on pure quartz sand that was filled in an empty sample segment with 2 M HCl. This allowed for a proper copy of the sample geometry and density. The efficiency curve is displayed in Fig. S1 in the Supporting Information.

2.4. Radiostrontium analysis

In contrast to the quite straightforward gamma spectrometry, the analysis of ^{90}Sr is quite laborious as it requires chemical separation of the Sr fraction from the sample matrix. The activity distribution was assumed to be exponential through the soil column, similar to radiocesium; due to the expected low activities of ^{90}Sr in the soil, only the top two layers (0 cm–2.5 cm and 2.5 cm–5 cm) were analyzed for ^{90}Sr. For a step-by-step description of the analytical procedure of Sr separation, please see Supporting Information or previous publications (Steinhauser et al., 2015). In brief, leaching of radionuclides (including ^{90}Sr and ^{60}Fe) from the surface of the soil particles was performed by boiling samples in HNO_3 and H_2O_2 under reflux for 30 min (4 mL 8 M HNO_3, 1 mL 1.2 mg mL^{-1} $Sr(NO_3)_2$ carrier solution, 1 mL 30% H_2O_2, 2 mL 16 M HNO_3). After filtration, the leachate was brought to 8 M HNO_3. The Sr fraction was separated from the solution by ion specific extraction chromatography (Eichrom® SR resin), and then counting the samples on the Hidex 300 SL Liquid Scintillation Counter using Perkin Elmer's® Ultima Gold™ scintillation cocktail. In order not to let natural radiolead interfere with the ^{90}Sr analysis, good care was taken to not co-elute ^{210,212}Pb from the SR columns during the separation by using 0.01 M HNO_3 as eluting agent (Kocadag et al., 2013).

For the LSC measurement, samples were dark-adapted for more than 2 h prior to measurement to minimize residual fluorescence within the scintillation cocktail. Measurements were conducted for 3 × 6000 s, with the first measurement discarded and latter two averaged. The reason for discarding the first measurement was that it allowed for adaption following mechanical disturbance and

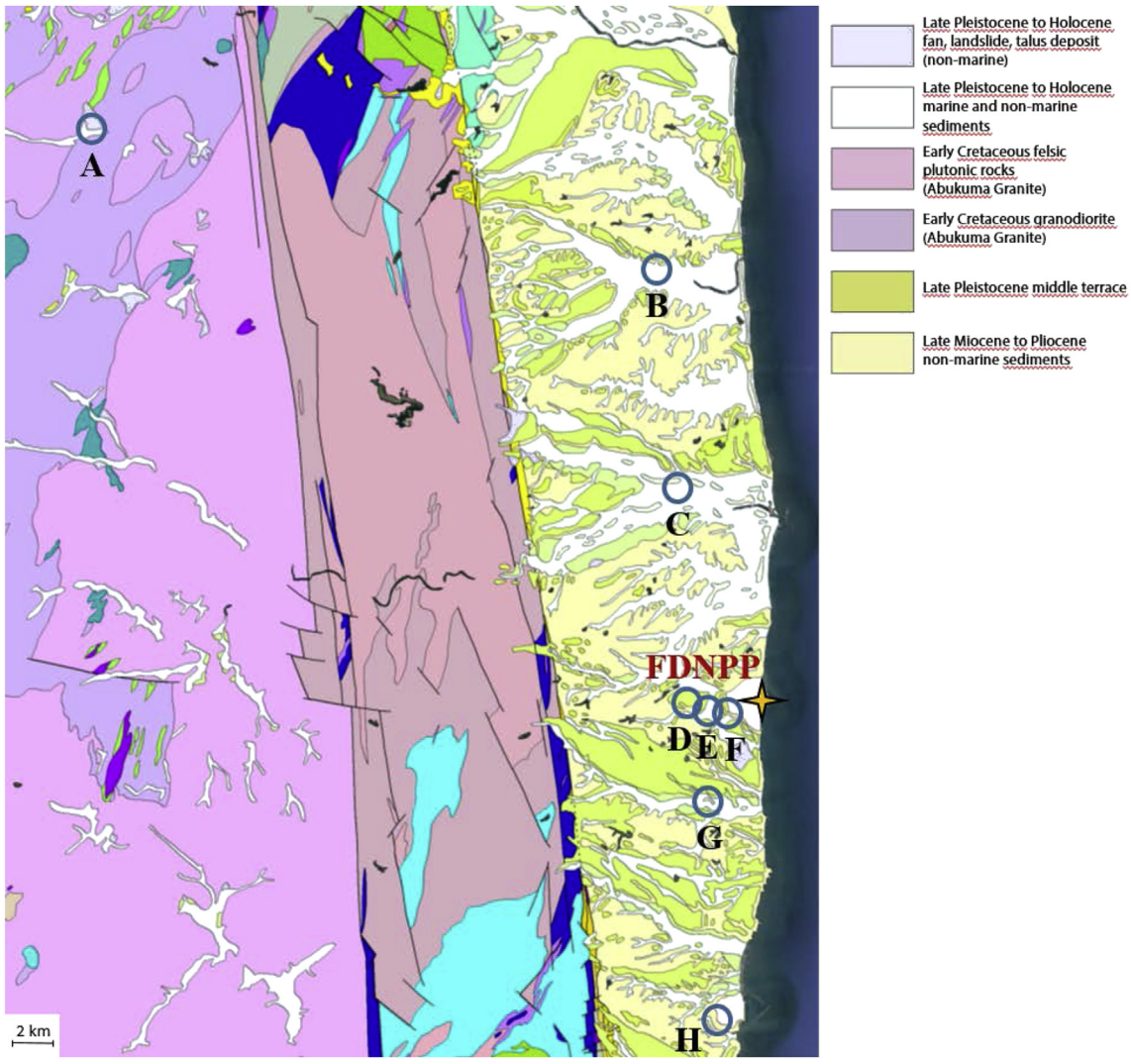

Fig. 1. Geological setting of the sampling locations around the Fukushima Daiichi NPP (indicated by the yellow star). Please refer to Table 1 for the site codes. The map was prepared based on a map provided online by the Geological Survey of Japan (Geological Survey of Japan, 2017). (For interpretation of the references to colour in this figure legend, the reader is referred to the web version of this article.)

electrostatic charges due to the movement of the plastic vial inside the LSC counter. For quality control purposes, all samples were measured twice. First, immediately after the radiochemical separation (with no or only little ingrowth of the short-lived radioactive daughter ^{90}Y). Then, samples were re-measured after approximately one month, when ^{90}Sr and its daughter ^{90}Y were in secular equilibrium. A total count rate that has doubled after background-subtraction would be indicative of ^{90}Sr and hence exclude any interferences, e.g., from trace of radiocesium.

The process efficiency for separation of ^{90}Sr from soil samples was established by gamma spectroscopy using a ^{85}Sr tracer on soil replicates. The efficiency for extraction from soil matrices was determined to be 88% by gamma spectroscopy. The absolute efficiency was evaluated by spiking 1.097 g IAEA ^{90}Sr Standard 373 into soil blanks with 1.2 mg stable Sr^{2+} carrier. The sample was subjected to the separation process and allowed to reach secular equilibrium. By using this sample and a background sample generated by extracting stable Sr^{2+} carrier from a soil sample, the absolute efficiency was determined to be 66%. (The detection efficiency can be calculated by dividing the absolute efficiency by the process efficiency, yielding 75%.). The analytical uncertainties in the analysis of ^{90}Sr are typically around 10% (rel.).

2.5. Tritium and radioiron analysis

A selection of interesting soil samples from 2013 were submitted to the accelerator mass spectrometry (AMS) facility at TU München, Germany, for ^{60}Fe analysis. For this pilot project, the samples with the highest (radiocesium) activities (2 samples from location **F** and one sample from location **E**) as well as from Minamisoma (**B**) (a location with some unusual radionuclide patterns (Schneider et al., 2013; Steinhauser et al., 2013, 2015)) were chosen, assuming that they will be the most likely to carry an ^{60}Fe signal. After the acidic leaching for the separation of the Sr fraction, the effluent from the SR resin was loaded directly onto Eichrom's TRU resin for iron separation. The TRU resin is highly specific for trivalent ions, including Fe(III). The use of this resin was necessary to suppress isobaric ^{60}Ni. After loading of the 8 M HNO_3 solution and elution with H_2O, the Fe(III) was precipitated with ammonia in the form of $Fe(OH)_3$. and further treated for AMS measurements as described elsewhere (Knie et al., 2000).

Tritium was distilled from soil and vegetation samples from the

sampling locations by placing them in a double-necked flask inside a furnace and combusting the organic material under a flow of dried air. The vapor was collected in a dry-ice-cooled trap and yielded a clear distillate that was measured by LSC using Perkin Elmer's® Ultima Gold LLT™ scintillation cocktail.

3. Results and discussion

3.1. Radiocesium and radiostrontium concentrations

Fig. 2 shows the depth profiles of activity concentrations of ^{137}Cs and ^{90}Sr, respectively, in the soil drill cores from 2013 to 2014. Since the cores taken in Iitate Village (**A**) and Fukushima Daini NPP (**H**) were only taken in 2013, they were omitted from these graphs. A full list of numerical analytical data is presented in Tables S3-S6 in the Supporting Information. Activities in Fig. 2 have been time-corrected to the date of sampling. The graphs show that most activity concentrations were higher in 2013 than 13 months later. However, some sampling sites exhibit a peculiar, different pattern (e.g., locations **E** and **G**). Such rather peculiar behavior is not explainable by diffusion or radioactive decay, but it may indicate later deposition of radionuclides by re-suspension of already deposited material (Hirose, 2013, 2015; Steinhauser et al., 2015) or simply inhomogeneous distribution even on a very small geographical scale. If the latter is true, it may simply indicate that repeated sampling (with little chances of exactly reproducing the sampling sites) may reveal such very local differences in activity concentrations. Within the core, the activity concentrations decreased with a near exponential decline for most samples. This behavior was also described in literature previously (Honda et al., 2015; Konoplev et al., 2016; Lepage et al., 2015; Matsuda et al., 2015; Walling and He, 1999). Samples collected from the Gate (**F**) and in Iitate Village (**A**) have exponential distributions of radiocesium, although the Gate sample from 2013 has a surface activity in excess of a value that would be extrapolated from the other layers. The higher activity in the top layer of the soil core from the gate may be a result of re-suspended radioactive material that has settled in that area. Some other sites, however, showed a different behavior as location **E** (and also one core of site **D**) exhibited a spike in radiocesium activity in deeper layers. This may be due to soil disturbances but also to an inhomogeneous distribution of radiocesium "granules" which may have been washed down to deeper layers (with little interaction with the minerals and organic constituents of the soil). These granules are extremely radioactive, sparingly soluble, and exhibit almost ceramic properties. If a segment should contain such highly radioactive particles, it may be interpreted as if the activity levels were generally higher in deeper layers.

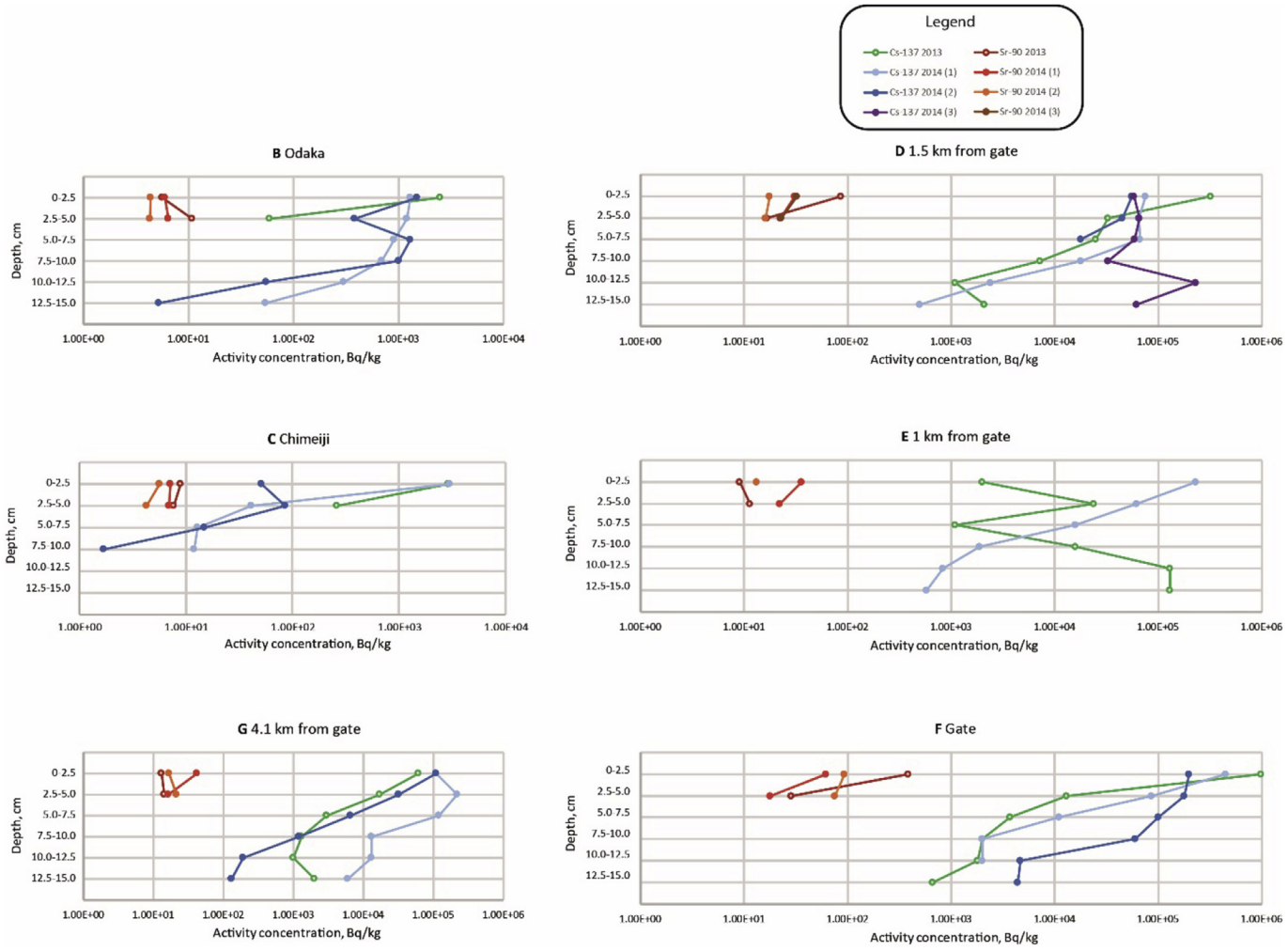

Fig. 2. Activity concentrations of ^{137}Cs (green and blue) and ^{90}Sr (red) (in Bq kg^{-1}) in layers of soil (cm) at the sampling locations of this study (except sites **A** and **H**) in 2013 and 2014. (For interpretation of the references to colour in this figure legend, the reader is referred to the web version of this article.)

Radiocesium activities did decrease between 2013 and 2014. Maximum activity concentrations of ^{137}Cs in soil were found in close vicinity of the gate of FDNPP and reached up to 10^6 Bq·kg^{-1} in 2013. Thirteen months later, these maximum levels were lower by a factor of at least 5. There are several differences, though, between samples from each year. In 2013, six of the eight soil cores had more than 90% of the radiocesium activity in the top five cm of soil. The sample from Iitate Village (**A**) and the soil core from 1 km from the gate (**E**) had 87% and 84% of the radiocesium activity in the top 5 cm, respectively. In 2014, five of the 12 soil cores had more than 90% of the radiocesium activity in the top 5 cm of soil. Two of these five samples were from the gate (**F**) and a core 4.1 km from the gate (**G**). The second cores from each of these two sites had less than 70% of the activity in the top 5 cm.

Strontium-90 concentrations were generally 3–4 orders of magnitude lower than the respective radiocesium concentrations

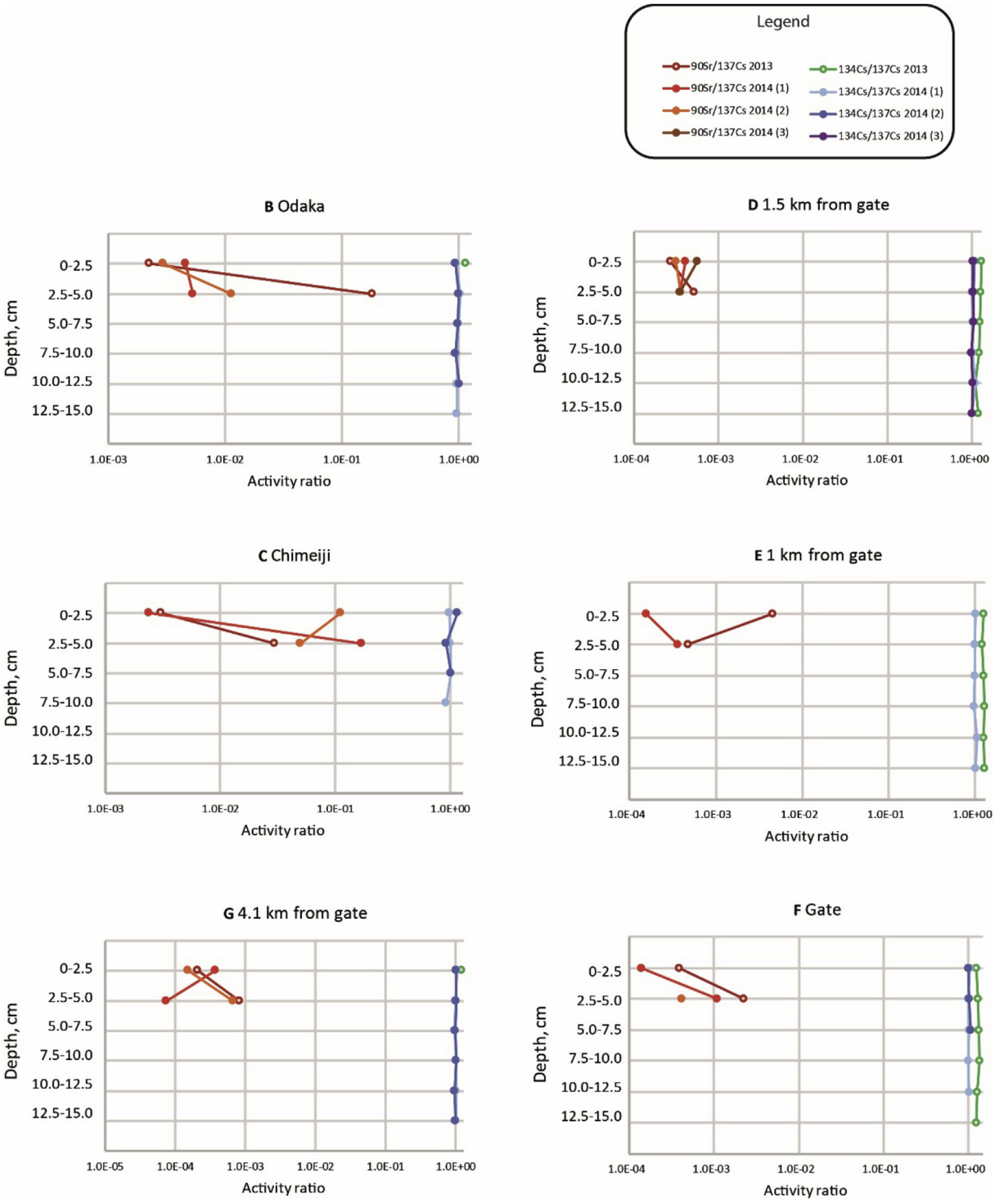

Fig. 3. Activity ratios of $^{134}Cs/^{137}Cs$ and $^{90}Sr/^{137}Cs$ (both decay corrected to the date of the accident) at the sampling locations of this study (except site **A** and **H**) in 2013 and 2014, respectively.

and did not exceed 10^3 Bq·kg^{-1}. The ^{90}Sr levels have declined significantly compared with the 2011 study (Steinhauser et al., 2013), where samples were taken in similar locations. No clear trend is visible with respect to sampling depth within the core. As expected, the semi-volatile radionuclide ^{90}Sr exhibits some dependency with distance to the FDNPP site: samples nearer to the FDNPP exhibit significantly higher activity concentrations.

Different specific activities within the layers are most likely due to migration within the soil column. Strontium has a weaker interaction with clay surfaces than the lighter alkaline earth metals Ca and Mg. Strontium also interacts with organic matter and forms water soluble complexes with low-molecular organic or fulvic acids. Irreversible sorption is only expected with minerals such as vermiculite, dolomite, magnetite, or calcite (Sokolik et al., 2001). Since Sr is thought to exhibit outer-sphere complexation behavior, this type of interaction with the clay surface could justify its more rapid movement through the soil column in comparison to Cs (Miller and Reitemeier, 1963; Rahnemaie et al., 2006).

3.2. ^{134}Cs/^{137}Cs and ^{90}Sr/^{137}Cs activity ratios

The activity ratios of ^{134}Cs/^{137}Cs and ^{90}Sr/^{137}Cs are displayed in Fig. 3.

Activity ratios of ^{134}Cs/^{137}Cs may reveal some forensic insight on the source of a contamination (Merz et al., 2013). For example, old radiocesium should not exhibit any detectable ^{134}Cs, hence the presence of this radionuclide is a clear indicator of the Fukushima nuclear accident. The ratios may also be used for quality control of the reliability of the measurement, as no major fluctuations of the ratio should occur in homogeneously contaminated samples. The ratios shown in Fig. 3 were decay-corrected to the time of the accident. Literature suggests activity ratios between 0.91 and 1.04, as found by (Komori et al., 2013) based on characterization of releases by the reactors. The samples in this study exhibited ratios mostly matching this “radiocesium fingerprint.” It is noteworthy, however, that the samples with a higher contamination level (sites D, E, and F) exhibited a slightly higher activity ratio than the lower contaminated samples, for which we currently do not have an explanation.

The activity ratios of ^{90}Sr/^{137}Cs indicate that all sites exhibited significantly higher radiocesium contaminations than ^{90}Sr contaminations. The ratios were typically between 10^{-4} and 10^{-2}, only some samples from Chimeiji (**C**) and Odaka (**B**) exhibited a^{90}Sr/^{137}Cs ratio in the range of 10^{-1}. It is possible that resuspended material from the FDNPP site has impacted the ratio and locally increased the ratio (Steinhauser et al., 2015); however, this is difficult to judge from the small number of samples taken in the area.

In many samples, the ^{90}Sr/^{137}Cs activity ratio increased with depth by up to one order of magnitude (sometimes even more). This may be the result of enhanced retention of Cs^+ ions in upper layers (interaction with clay minerals), whereas Sr^{2+} ions remain mobile. This phenomenon, however, was not observed consistently even with multiple samples taken at the same location. Since, after the decay of short-lived ^{89}Sr, there is no isotopic sentinel left for Sr (indicating the contribution from Fukushima), a small amount of ^{90}Sr may also originate from previous sources such as the fallout from atmospheric nuclear explosions in the 20th century (several thousands of Bq/m^2) (Guillén et al., 2010).

3.3. Tritium and iron-60 measurements

In this pilot study, no significantly increased levels of tritium could be observed in any of the vegetation samples taken in 2013. This confirms the very high mobility of tritium in the environment and the effective dilution after the releases in 2011. The lack of a detectable ^{3}H increase also indicates that, despite media reports covering the leaks at the water tanks at the FDNPP site, the environmental inventory of tritium in the area has not significantly increased.

Iron-60 was also not found in any of the samples investigated by AMS. The samples did not reveal any increase of the blank (^{60}Fe/Fe ~8×10^{-17}). This indicates that no iron was released from the reactors that was exposed to a high neutron flux (e.g., scaling on the surface of the fuel rods) in the course of the accident. Iron-59 released from the reactors (Shozugawa et al., 2012) was probably activated in a lower neutron flux density (e.g., the pressure vessel) than what would have been necessary to cause double neutron capture and formation of ^{60}Fe.

4. Conclusions

Radiocesium was present in Fukushima exclusion zone soil with activity levels up to 1 MBq/kg in 2013. Although these levels generally decreased in comparison with the next set of samples taken in 2014, we observed some inconsistent migration pattern that is not yet fully explainable. Some samples showed increasing activity concentrations at certain depths. One possible explanation for this phenomenon is resuspension with highly radioactive particles from the NPP site. In any case, the general downward trend was confirmed by dose rate measurements along the sampling route in both years. Activity ratios of ^{134}Cs/^{137}Cs were shown to be a little higher for most spots than the expected value of approximately 1 (when decay corrected to March 11, 2011). This may indicate, (1) that the releases from the reactors were not totally homogenous with respect to the isotopic composition of the radiocesium fraction and (2) that the contribution of “old” fallout ^{137}Cs is negligible.

In contrast to radiocesium, radiostrontium concentrations in soil from the Fukushima exclusion zone in most cases showed a significant decline from 2013 to 2014: from a maximum concentration of almost 400 Bq/kg in 2013 (sample taken at the gate of Fukushima Daiichi NPP), the soil sampled in 2014 at the same location exhibited less than 100 Bq/kg ^{90}Sr.

Tritium above background levels was not detected in soil and vegetation samples. Detectable activity of ^{60}Fe was not found in soil extracts.

Acknowledgements

This study was supported by JSPS KAKENHI (Grant Number 25870158) as well as Grant Number T42OH009229-07 from CDC NIOSH Mountain and Plains Education and Research Center. Its contents are solely the responsibility of the authors and do not necessarily represent the official views of the CDC NIOSH and MAP ERC. GS gratefully acknowledges funding by the US Nuclear Regulatory Commission (NRC), grant number NRC-HQ-12-G-38-0044.

Appendix A. Supplementary data

Supplementary data related to this article can be found at http://dx.doi.org/10.1016/j.apgeochem.2017.06.003.

References

Benedicto, A., Missana, T., Fernández, A.M., 2014. Interlayer collapse affects on cesium adsorption onto illite. Environ. Sci. Technol. 48, 4909–4915.
Bostick, B.C., Vairavamurthy, M.A., Karthikeyan, K.G., Chorover, J., 2002. Cesium adsorption on clay Minerals: an EXAFS spectroscopic investigation. Environ. Sci. Technol. 36, 2670–2676.
Casacuberta, N., Masque, P., Garcia-Orellana, J., Garcia-Tenorio, R., Buesseler, K.O.,

2013. ^{90}Sr and ^{89}Sr in seawater off Japan as a consequence of the Fukushima Dai-ichi nuclear accident. Biogeosciences 10, 3649–3659, 3611 pp.
Coleman, N.T., Lewis, R.J., Craig, D., 1963. Sorption of cesium by soils and its displacement by salt solutions. Soil Sci. Soc. Am. J. 27, 290–294.
Davey, P.T., Scott, T.R., 1956. Adsorption of uranium on clay minerals. Nature 178, 1195–1195.
Dawood, Y.H., Abd El-Naby, H.H., 2001. Mineralogy and genesis of secondary uranium deposits, Um Ara area, south eastern desert, Egypt. J. Afr. Earth Sci. 32, 317–323.
Essington, M.E., 2005. Soil and Water Chemistry: an Integrative Approach. CRC Press LLC, Boca Raton.
Fujimoto, K., Miki, S., Kaeriyama, H., Shigenobu, Y., Takagi, K., Ambe, D., Ono, T., Watanabe, T., Morinaga, K., Nakata, K., Morita, T., 2015. Use of otolith for detecting Strontium-90 in fish from the harbor of Fukushima Dai-ichi nuclear power plant. Environ. Sci. Technol. 49, 7294–7301.
Geological Survey of Japan, 2017. Geological Map of Japan (Accessed March 2017). https://gbank.gsj.jp/geonavi/geonavi.php#12,37.48901,140.89869.
Guillén, F.J., Baeza, A., Salas, A., 2010. Strontium. In: Atwood, D.A. (Ed.), Radionuclides in the Environment. John Wiley & Sons, Chichester.
Hamada, N., Ogino, H., 2012. Food safety regulations: what we learned from the Fukushima nuclear accident. J. Environ. Radioact. 111, 83–99.
Hashimoto, S., Matsuura, T., Nanko, K., Linkov, I., Shaw, G., Kaneko, S., 2013. Predicted spatio-temporal dynamics of radiocesium deposited onto forests following the Fukushima nuclear accident. Sci. Rep. 3, 2564.
Hirose, K., 2013. Temporal variation of monthly ^{137}Cs deposition observed in Japan: effects of the Fukushima Daiichi nuclear power plant accident. Appl. Radiat. Isot. 81, 325–329.
Hirose, K., 2015. Two-years trend of monthly ^{137}Cs deposition observed in Kanto and south Tohoku areas, Japan: effects of the Fukushima Dai-ichi nuclear power plant accident. J. Radioanal. Nucl. Chem. 303, 1327–1329.
Honda, M., Matsuzaki, H., Miyake, Y., Maejima, Y., Yamagata, T., Nagai, H., 2015. Depth profile and mobility of ^{129}I and ^{137}Cs in soil originating from the Fukushima Dai-ichi nuclear power plant accident. J. Environ. Radioact. 146, 35–43.
Jeong, C.H., Kim, C.S., Kim, S.J., Park, S.W., 1996. Affinity of radioactive cesium and strontium for illite and smectite clay in the presence of groundwater ions. J. Environ. Sci. Health. Part A Environ. Sci. Eng. Toxicol. 31, 2173–2192.
Kakiuchi, H., Akata, N., Hasegawa, H., Ueda, S., Tokonami, S., Yamada, M., Hosoda, M., Sorimachi, A., Tazoe, H., Noda, K., Hisamatsu, S., 2012. Concentration of ^{3}H in plants around Fukushima Dai-ichi nuclear power station. Sci. Rep. 2, 947.
Kavasi, N., Sahoo, S.K., Sorimachi, A., Tokonami, S., Aono, T., Yoshida, S., 2015. Measurement of ^{90}Sr in soil samples affected by the Fukushima Daiichi nuclear power plant accident. J. Radioanal. Nucl. Chem. 303, 2565–2570.
Kim, Y., Cho, S., Kang, H.-D., Kim, W., Lee, H.-R., Doh, S.-H., Kim, K., Yun, S.-G., Kim, D.-S., Jeong, G.Y., 2006. Radiocesium reaction with illite and organic matter in marine sediment. Mar. Pollut. Bull. 52, 659–665.
Kinoshita, N., Sueki, K., Sasa, K., Kitagawa, J.-I., Ikarashi, S., Nishimura, T., Wong, Y.-S., Satou, Y., Handa, K., Takahashi, T., Sato, M., Yamagata, T., 2011. Assessment of individual radionuclide distributions from the Fukushima nuclear accident covering central-east Japan. Proc. Natl. Acad. Sci. U. S. A. 108, 19526–19529.
Knie, K., Faestermann, T., Korschinek, G., Rugel, G., Rühm, W., Wallner, C., 2000. High-sensitivity AMS for heavy nuclides at the Munich Tandem accelerator. Nucl. Instrum. Meth. B 172, 717–720.
Koarashi, J., Atarashi-Andoh, M., Amano, H., Matsunaga, T., 2017. Vertical distributions of global fallout ^{137}Cs and ^{14}C in a Japanese forest soil profile and their implications for the fate and migration processes of Fukushima-derived ^{137}Cs. J. Radioanal. Nucl. Chem. 311, 473–481.
Koarashi, J., Atarashi-Andoh, M., Matsunaga, T., Sato, T., Nagao, S., Nagai, H., 2012a. Factors affecting vertical distribution of Fukushima accident-derived radiocesium in soil under different land-use conditions. Sci. Total Environ. 431, 392–401.
Koarashi, J., Moriya, K., Atarashi-Andoh, M., Matsunaga, T., Fujita, H., Nagaoka, M., 2012b. Retention of potentially mobile radiocesium in forest surface soils affected by the Fukushima nuclear accident. Sci. Rep. 2, 1005.
Kocadag, M., Musilek, A., Steinhauser, G., 2013. On the interference of ^{210}Pb in the determination of ^{90}Sr using a strontium specific resin. Nucl. Technol. Radiat. Prot. 28, 163–168.
Komori, M., Shozugawa, K., Nogawa, N., Matsuo, M., 2013. Evaluation ot radioactive contamination caused by each plant of Fukushima Daiichi Nuclear Power Station using ^{134}Cs/^{137}Cs activity ratio as an index. Bunseki Kagaku 62, 475–483.
Konoplev, A., Golosov, V., Laptev, G., Nanba, K., Onda, Y., Takase, T., Wakiyama, Y., Yoshimura, K., 2016. Behavior of accidentally released radiocesium in soil–-water environment: looking at Fukushima from a Chernobyl perspective. J. Environ. Radioact. 151, 568–578. Part 3.
Kubota, T., Shibahara, Y., Fukutani, S., Fujii, T., Ohta, T., Kowatari, M., Mizuno, S., Takamiya, K., Yamana, H., 2015. Cherenkov counting of ^{90}Sr and ^{90}Y in bark and leaf samples collected around Fukushima Daiichi nuclear power plant. J. Radioanal. Nucl. Chem. 303, 39–46.
Lepage, H., Evrard, O., Onda, Y., Lefèvre, I., Laceby, J.P., Ayrault, S., 2015. Depth distribution of cesium-137 in paddy fields across the Fukushima pollution plume in 2013. J. Environ. Radioact. 147, 157–164.
Matsuda, N., Mikami, S., Shimoura, S., Takahashi, J., Nakano, M., Shimada, K., Uno, K., Hagiwara, S., Saito, K., 2015. Depth profiles of radioactive cesium in soil using a scraper plate over a wide area surrounding the Fukushima Dai-ichi nuclear power plant. Jpn. J. Environ. Radioact. 139, 427–434.
Matsumoto, T., Maruoka, T., Shimoda, G., Obata, H., Kagi, H., Suzuki, K., Yamamoto, K., Mitsuguchi, T., Hagino, K., Tomioka, N., Sambandam, C., Brummer, D., Klaus, P.M., Aggarwal, P., 2013. Tritium in Japanese precipitation following the March 2011 Fukushima Daiichi nuclear plant accident. Sci. Total Environ. 445-446, 365–370.
Matsunaga, T., Koarashi, J., Atarashi-Andoh, M., Nagao, S., Sato, T., Nagai, H., 2013. Comparison of the vertical distributions of Fukushima nuclear accident radiocesium in soil before and after the first rainy season, with physicochemical and mineralogical interpretations. Sci. Total Environ. 447, 301–314.
Merz, S., Shozugawa, K., Steinhauser, G., 2015. Analysis of Japanese radionuclide monitoring data of food before and after the Fukushima nuclear accident. Environ. Sci. Technol. 49, 2875–2885.
Merz, S., Steinhauser, G., Hamada, N., 2013. Anthropogenic radionuclides in Japanese food: environmental and legal implications. Environ. Sci. Technol. 47, 1248–1256.
Miller, J.R., Reitemeier, R.F., 1963. The leaching of radiostrontium and radiocesium through Soils1. Soil Sci. Soc. Am. J. 27, 141–144.
Nakanishi, T., Matsunaga, T., Koarashi, J., Atarashi-Andoh, M., 2014. ^{137}Cs vertical migration in a deciduous forest soil following the Fukushima Dai-ichi Nuclear Power Plant accident. J. Environ. Radioact. 128, 9–14.
Normile, D., 2014. The trouble with tritium. Science 346, 1278.
Ota, M., Nagai, H., Koarashi, J., 2016. Modeling dynamics of ^{137}Cs in forest surface environments: application to a contaminated forest site near Fukushima and assessment of potential impacts of soil organic matter interactions. Sci. Total Environ. 551–552, 590–604.
Povinec, P.P., Hirose, K., Aoyama, M., 2012. Radiostrontium in the western north pacific: characteristics, behavior, and the Fukushima impact. Environ. Sci. Technol. 46, 10356–10363.
Rahnemaie, R., Hiemstra, T., van Riemsdijk, W.H., 2006. Inner- and outer-sphere complexation of ions at the goethite–solution interface. J. Colloid Interface Sci. 297, 379–388.
Rosso, K.M., Rustad, J.R., Bylaska, E.J., 2001. The Cs/K exchange in muscovite interlayers: an Ab initio treatment. Clays Clay Min. 49, 500–513.
Saito, K., Tanihata, I., Fujiwara, M., Saito, T., Shimoura, S., Otsuka, T., Onda, Y., Hoshi, M., Ikeuchi, Y., Takahashi, F., Kinouchi, N., Saegusa, J., Seki, A., Takemiya, H., Shibata, T., 2015. Detailed deposition density maps constructed by large-scale soil sampling for gamma-ray emitting radioactive nuclides from the Fukushima Dai-ichi Nuclear Power Plant accident. J. Environ. Radioact. 139, 308–319.
Schneider, S., Walther, C., Bister, S., Schauer, V., Christl, M., Synal, H.-A., Shozugawa, K., Steinhauser, G., 2013. Plutonium release from Fukushima Daiichi fosters the need for more detailed investigations. Sci. Rep. 3, 2988.
Shozugawa, K., Nogawa, N., Matsuo, M., 2012. Deposition of fission and activation products after the Fukushima Dai-ichi nuclear power plant accident. Environ. Pollut. 163, 243–247.
Shozugawa, K., Riebe, B., Walther, C., Brandl, A., Steinhauser, G., 2016. Fukushima-derived radionuclides in sediments of the Japanese Pacific Ocean coast and various Japanese water samples (seawater, tap water, and coolant water of Fukushima Daiichi reactor unit 5). J. Radioanal. Nucl. Chem. 307, 1787–1793.
Sokolik, G.A., Ivanova, T.G., Leinova, S.L., Ovsiannikova, S.V., Kimlenko, I.M., 2001. Migration ability of radionuclides in soil-vegetation cover of Belarus after Chernobyl accident. Environ. Int. 26, 183–187.
Steinhauser, G., 2014. Fukushima's forgotten radionuclides: a review of the understudied radioactive emissions. Environ. Sci. Technol. 48, 4649–4663.
Steinhauser, G., Bichler, M., 2008. Adsorption of ions onto high silica volcanic glass. Appl. Radiat. Isot. 66, 1–8.
Steinhauser, G., Brandl, A., Johnson, T.E., 2014. Comparison of the Chernobyl and Fukushima nuclear accidents: a review of the environmental impacts. Sci. Total Environ. 470–471, 800–817.
Steinhauser, G., Niisoe, T., Harada, K.H., Shozugawa, K., Schneider, S., Synal, H.-A., Walther, C., Christl, M., Nanba, K., Ishikawa, H., Koizumi, A., 2015. Post-accident sporadic releases of airborne radionuclides from the Fukushima Daiichi nuclear power plant site. Environ. Sci. Technol. 49, 14028–14035.
Steinhauser, G., Schauer, V., Shozugawa, K., 2013. Concentration of strontium-90 at selected hot spots in Japan. PLoS One 8, e57760.
Tanaka, K., Shimada, A., Hoshi, A., Yasuda, M., Ozawa, M., Kameo, Y., 2014. Radiochemical analysis of rubble and trees collected from Fukushima Daiichi nuclear power station. J. Nucl. Sci. Technol. 51, 1032–1043.
TU Munich, 1997. 1997 Annual Report (Accessed May 2017). http://www-old.mll-muenchen.de/bl_rep/jb1997/index.html.
Walling, D.E., He, Q., 1999. Improved models for estimating soil erosion rates from Cesium-137 measurements. J. Environ. Qual. 28, 611–622.
Yamamoto, T., 2012. Radioactivity of fission product and heavy nuclides deposited on soil in Fukushima Dai-Ichi Nuclear Power Plant accident. J. Nucl. Sci. Technol. 49, 1116–1133.
Yasunari, T.J., Stohl, A., Hayano, R.S., Burkhart, J.F., Eckhardt, S., Yasunari, T., 2011. Cesium-137 deposition and contamination of Japanese soils due to the Fukushima nuclear accident. Proc. Natl. Acad. Sci. U. S. A. 108, 19530–19534.
Yoshida, N., Takahashi, Y., 2012. Land-surface contamination by radionuclides from the Fukushima Daiichi nuclear power plant accident. Elements 8, 201–206.
Zaunbrecher, L.K., Cygan, R.T., Elliott, W.C., 2015. Molecular models of cesium and rubidium adsorption on weathered micaceous minerals. J. Phys. Chem. A 119, 5691–5700.